Expanded View Figures

Figure EV1. Killifish hearts show molecular, physiological and metabolic signatures of cardiac ageing.

A Immunohistochemistry on 10 μm cryosections of young (6 weeks) and aged (12 weeks) killifish ventricular tissue with cardiac marker MF-20. Cardiomyocyte sarcomeres are labelled with MF-20 (red).

B Kaplan–Meier analysis representing the survival of GRZ-AD killifish strain used in this study. The median lifespan of killifish in laboratory condition is ~ 9.5 weeks, indicated as stripped line (n = 170).

C Lipofuscin staining by Sudan Black B on 5 μm paraffin sections of different ages of killifish heart. Lipofuscin granules are labelled in grey-black colour. The bar graph on right represents the percentage area of the ventricular region acquired by lipofuscin granule with respect to total tissue area. Quantification was performed on a total of 12 sections per condition, covering independent regions of the ventricle. Number of animals = 3 per condition. Insets represent magnified view of the ventricles.

D Senescence detection based on SA-beta-galactosidase activity in ageing killifish hearts. Blue/cyan colour represents the positive regions in the ventricular sections. The bar graph on right represents percentage of SA-β-GAL-stained area with respect to the total ventricle area. Quantification was performed on a total of 12 sections per condition, covering different regions of the ventricle. Number of animals = 4 per condition. Insets represent magnified view of the ventricle.

E Principal component analysis of all the metabolites detected in various tissue samples. Number of animals = 4 per condition.

F Venn diagram of all the detected metabolites by untargeted metabolomics. Number of animals = 4 per condition.

G Bar graph depiction of the relative abundance of sphinganine levels in various killifish tissues obtained from untargeted metabolomics n = 4, each condition. Log_2 fold enrichment represents the relative abundance of sphinganine in aged tissues in comparison with young ones.

H Graphical illustration of collision-induced dissociation of standard sphinganine d18:0, resulted in 2 qualifiers and 1 quantifier. Mass by charge ratios (m/z) of corresponding fragments are mentioned underneath.

I Spectral peaks of both qualifiers (in red and green) and a quantifier (in blue) obtained from dissociation of standard sphinganine and of aged heart tissues from killifish, zebrafish, mouse and humans.

J Bar graph depicting the number of up and downregulated genes in the killifish ventricles upon ageing (n = 3 animals per condition).

K Transcriptional drift variance of all the detected transcripts in young and aged killifish hearts. Data are represented as box-plot, and Levene's test was used for the estimation of the statistical significance. Error bars represent drift-variance. Box plot whiskers show 1.5 IQR of highest and lowest quartile. Horizontal line within the bars represent median of the underlying population.

L Heatmap representation of the hallmark genes of sphingolipid metabolism and DNA damage pathways shows differential expression in young and aged killifish hearts. Scale bar represents scaled FPKM (Fragments Per Kilobase of transcript per Million mapped reads), to graphically represent expression levels of the indicated genes, on a scale given scale.

M Micrographs of comet assay on isolated killifish cardiomyocytes from young and old individuals n = 4, each condition.

N Bar graph illustrating the absolute transcript expression of ceramide synthase 2 between young and aged killifish ventricles, n = 3 per condition. Expression levels are depicted in FPKM (Fragments Per Kilobase of transcript per Million mapped reads).

O Heatmap with scaled FPKM values of all detected histone deacetylase genes, which are differentially expressed in the killifish transcriptome. Scale bar represents scaled FPKM, to graphically represent expression levels of the indicated genes on a scale given scale.

Data information: When not specified, the experiments were conducted in at least three biological replicates. Error bars in panels (C, D and N) represent standard error of the mean. For pairwise comparisons, Student's t-test was performed for the estimation of the statistical significance. P-value cut-off used for computing statistical significance is < 0.05. *, ** and **** in the figure refer to P-values ≤ 0.05, ≤ 0.01 and ≤ 0.0001, respectively. Statistically non-significant comparisons are annotated as ns. Scale bars = 50 μm.

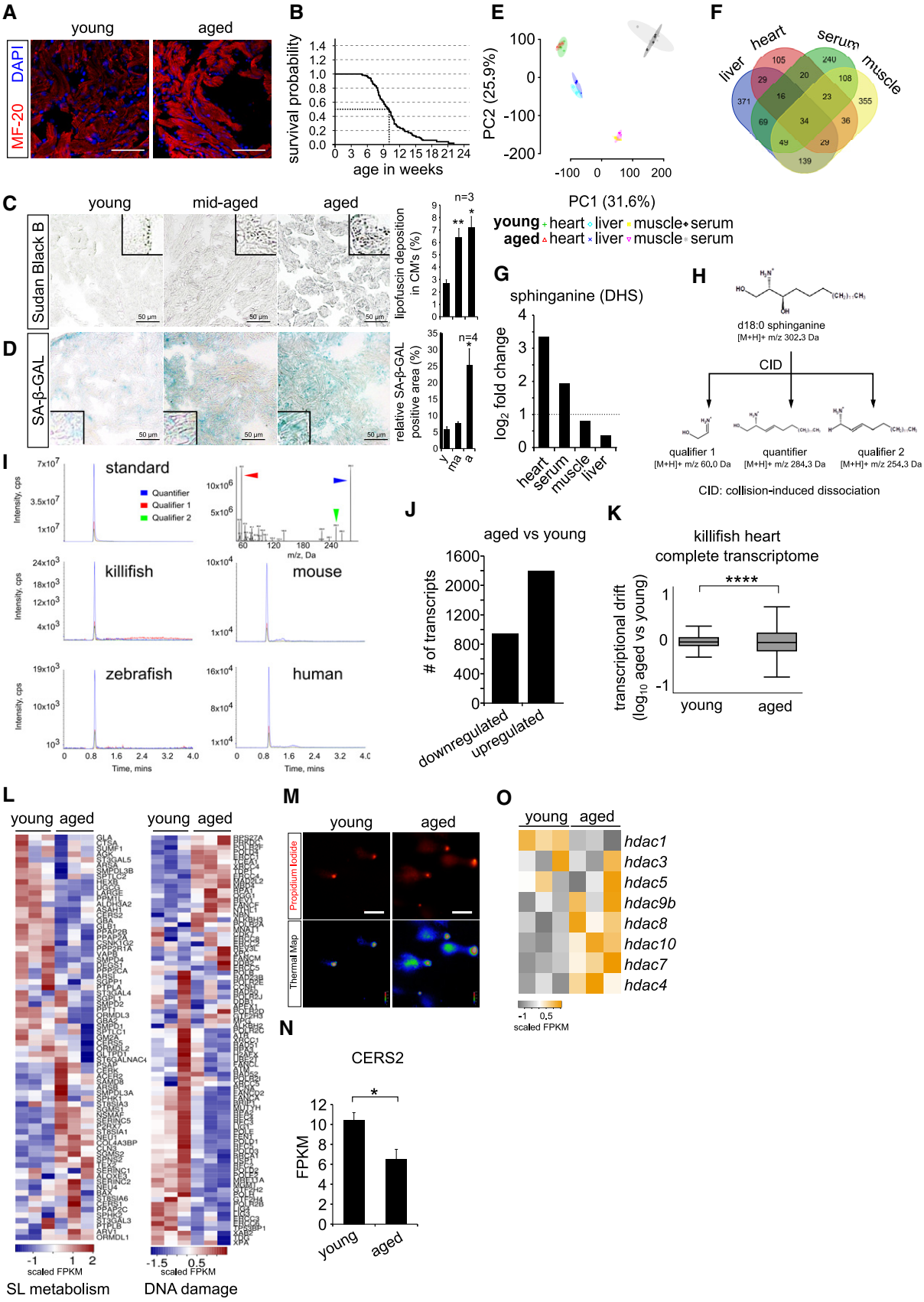

Figure EV1.

Figure EV2. Elevated sphinganine levels induce DNA damage without causing apoptosis in cardiomyocytes.

A Human pluripotent stem cell-derived cardiomyocytes (hCMs) express ventricle-specific marker MYL2 (red); insets show a magnified single cardiomyocyte.

B Calcium response in post-mitotic hCMs. Left and right panel depicts basal and excitation states of hCMs, respectively.

C Graphical depiction of ratiometric measurement of fluorescence from different ROI (region of interest). Fluorescence intensities from the indicated ROIs (faint red circles) were measured (F) and normalized to basal fluorescence levels (Fo). The normalized data points (F/Fo) were plotted over time.

D Heatmap depicting expression profile of early and late cardiomyocytes markers during key time points of differentiation. CP (cardiac progenitors), ehCMs (early human cardiomyocytes) and hCMs (human cardiomyocytes). Scale bar represents scaled FPKM, to graphically represent expression levels of the indicated genes, on a scale of −1 to +1.

E Exogenous treatment of hCMs with 10 μM DHS leads to significant increase in intracellular DHS levels in comparison with DMSO control. Experiment was performed in biological triplicate.

F Dose-dependent increase in γH2A.X$^+$ nuclear foci in hCMs upon DHS exposure. hCMs were pre-incubated for 3 days with either 1, 5 μM or 10 μM of DHS. The graph on the right represents quantifications from n = 3 experiments. ACTN2 is used to specifically label human cardiomyocytes (red).

G Elevated DHS levels induce DNA damage in hCMs but not in human primary fibroblasts shown here by immunostaining for γH2A.X (green). Bar graph on the right represents percentage of γH2A.X$^+$ positive nuclei per condition. These experiments were performed in biological triplicate, and a total of ~ 170 cells were quantified.

H Human cardiomyocytes were pre-incubated for 3 days with either DMSO, 10 μM Fumonisin B1 or 10 μM sphinganine (DHS), and the induction of DNA damage was assayed by immunostaining for γH2A.X (green). Bar graph to the right depicts the percentage of γH2A.X positive nuclei in the indicated conditions. (n = 3 biological replicates; number of cells quantified per replicate = 150–200). ACTN2 is used to specifically label human cardiomyocytes (red).

I Representative micrographs depicting the results of comet assay in the indicated conditions.

J Chronic exposure of hCMs with lower concentrations of sphinganine (0.01 and 0.1 μM) for 7 days induces signs of DNA damage shown here by γH2A.X immunostaining. Bar graph represents percentage of positive nuclei per condition.

K Elevated DHS levels cause apoptosis in human primary fibroblasts but not in hCMs shown here by immunostaining with active caspase-3 (green). White arrowheads indicate the active caspase-3-stained regions. Bar graph on the right represents percentage of active caspase-3-positive cells in the indicated conditions. Experiment was performed in biological triplicate, and a total of ~ 150 cells were quantified per condition.

Data information: When not specified, the experiments were conducted in at least three biological replicates. Error bars in panel (E, F, G, H, J and K) represent standard error of the mean. For pairwise comparisons, Student's t-test was performed for the estimation of the statistical significance. P-value cut-off used for computing statistical significance is < 0.05. * and ** in the figure refer to P-values ≤ 0.05 and ≤ 0.01, respectively. Statistically non-significant comparisons are annotated as ns. Scale bars = 10 μm, except for panel (I) 50 μm and for insets 5 μm.

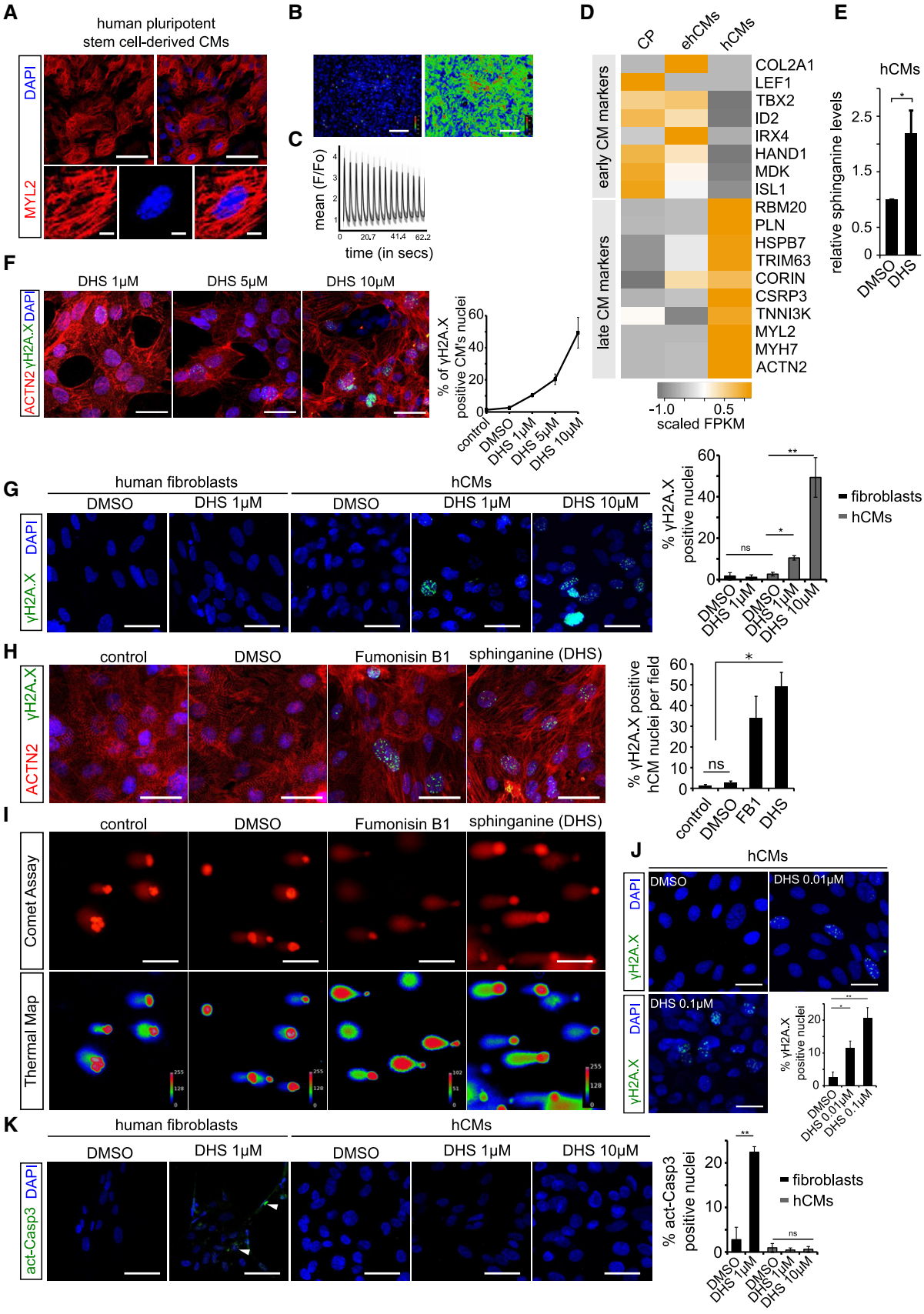

Figure EV2.

Figure EV3. Elevated sphinganine levels induce genomic instability and ageing signatures in human cardiomyocytes.

A Elevated DHS levels in hCMs induce signature of cellular senescence indicated here by representative micrographs from SA-beta-galactosidase staining (blue/cyan colour represents the positive regions). Arrowheads in the representative panels indicate the SA-beta-galactosidase-stained regions.

B Elevated DHS levels in hCMs induce p21 expression indicated here by representative micrographs from p21 immunostaining (in green). ACTN2 is used to specifically label human cardiomyocytes.

C Violin plot depicting the distributions of the greyscale nuclear intensity of the indicated markers. n = 3 biological replicates; number of fields evaluated per condition = 12; total number of cells quantified per replicate = 150–200).

D Bar graph representing the percentage of hCMs nuclei harbouring elevated p21 levels. n = 3 biological replicates; number of fields evaluated per condition = 12; total number of cells quantified per replicate = 150–200).

E Elevated DHS levels lead to HP1-α^+ nuclear loci in hCMs. MYL2 is used to specifically label cardiomyocytes (red).

F Bar graph depicting the percentage positive nuclei HP1-α foci in human cardiomyocytes (n = 3 biological replicates; number of fields evaluated per condition = 9; number of cells quantified per replicate = 120–200).

G Violin plot depicting the distributions of the greyscale nuclear intensity of the indicated markers (n = 3 biological replicates; number of fields evaluated per condition = 9; number of cells quantified per replicate = 120–200).

H DHS exposure leads to significant increase in H4K16ac (in red) levels accompanied by nuclear envelope defects (Lamin B1 immunostaining in green) of cardiomyocytes.

I Violin plot depicting the distributions of the greyscale nuclear intensity of the indicated marker (n = 3 biological replicates; number of cells quantified per replicate = 100–150).

J Heatmap depicting the relative enrichment/de-enrichment of the indicated proteins as inferred from label-free proteomics analysis.

K Western blot analysis revealed decreased levels of HDAC1 protein in the DHS-treated human cardiomyocytes. Quantifications are on the right.

L DHS exposure of hCMs does not alter the levels of H3K27me3 and H3K9me3. ACTN2 or MYL2 is used to specifically label human cardiomyocytes.

M Box-plot representing the normalized nuclear intensities of H3K27me3 and H3K9me3. Extremes of the error bars represent non-outlier range, and their length represents the variability within the data. Horizontal line within the bars represents median of the underlying population. Box plot whiskers show 1.5 IQR of highest and lowest quartile, outliers are included (dots). Extremes of the error bars represent non-outlier range and their length represents the variability within the data. Horizontal line within the bars represent median of the underlying population.

N Bar graphs representing the decline in the transcript levels of hdac1a (left) and hdac1b (right) in the killifish ventricles as inferred by RT–qPCR. X-axis represents fish age in weeks (annotated as W).

Data information: When not specified, the experiments were conducted in at least three biological replicates. Error bars in panels (D, F, K and N) represent standard error of the mean. Panels (C, D, F, G and I) share the same x-axis legend (conditions). For pairwise comparisons, Student's t-test was performed for the estimation of the statistical significance. For the comparison of fluorescence signal intensities (panels C, G, I and M), KS-test was used as a measure of statistical significance. P-value cut-off used for computing statistical significance is < 0.05. * and ** in the figure refer to P-values ≤ 0.05 and ≤ 0.01, respectively. Statistically non-significant comparisons are annotated as ns. Scale bars = 10 μm except for panel (L) = 20 μm.

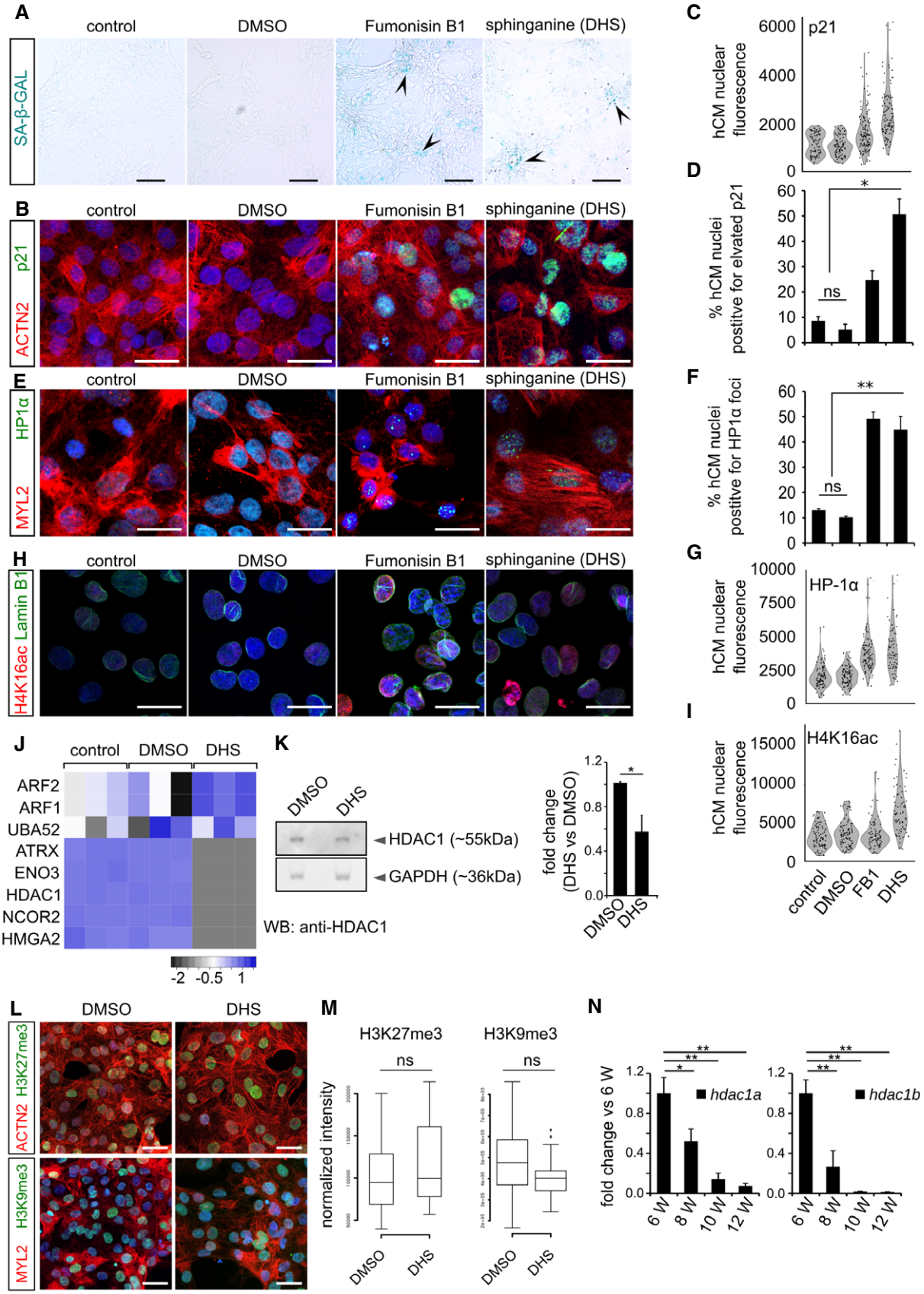

Figure EV3.

Figure EV4. DHS-induced genomic instability is a consequence of HDAC inhibition in human cardiomyocytes.

A Elevated DHS levels in hCMs do not affect mitochondrial network and its membrane potential. Co-staining of mitochondria by MitoTracker (in green) along with the cardiac-specific marker ACTN2 (in red).

B Micrographs of live cell imaging of hCMs stained with MitoTracker (in red).

C Bar graph representing the corrected total fluorescence mean ± SEM, from live cardiomyocytes stained with MitoTracker $n = 3$, each condition.

D Elevated DHS levels do not increase the ROS levels in human cardiomyocytes. Measurement of reactive oxygen species (ROS) in hCMs pre-incubated for 72 h with DMSO, DHS, ROS inhibitors, rotenone and DHS + ROS inhibitors.

E Elevated DHS levels induce ROS-independent DNA damage as shown by immunostaining with γH2A.X (in green).

F Molecular docking of human HDAC1 protein with Trichostatin TSA, a pan HDAC inhibitor, suggests potential binding within the known active site pocket (spotted square and the magnified view of the active site is to the right). TSA and HDAC1 are represented in ball & stick and spacefill models, respectively.

G Ligplot representing the two-dimensional interaction between the HDAC1 residues with TSA at the active site.

H Cardiac sphingosine levels remain unchanged with age *in vivo* in mice. Bar graph depicting the relative sphingosine (Spo) levels in aged mouse hearts in comparison with the young ones.

I Exogenous treatment of hCMs with 10 μM DHS did not alter sphingosine (Spo) levels, depicted as a bar graph in comparison with DMSO control. Experiment was performed in biological triplicate.

J Concentration curves depicting the comparable IC50 values of DHS1P and S1P from in cellulo HDAC assay.

K Box-plot depicting the normalized nuclear (without nucleolus) intensities of nascent transcript, measured by EU labelling. Extremes of the error bars represent non-outlier range, and their length represents the variability within the data. Horizontal line within the bars represents median of the underlying population. Box plot whiskers show 1.5 IQR of highest and lowest quartile, outliers are included (dots). Extremes of the error bars represent non-outlier range and their length represents the variability within the data. Horizontal line within the bars represent median of the underlying population, respectively.

Data information: When not specified, the experiments were conducted in at least three biological replicates. Error bars in panels (C, H and I) represent standard error of the mean. For pairwise comparisons, Student's *t*-test was performed for the estimation of the statistical significance. For the comparison of fluorescence signal intensities (panels H and I), KS-test was used as a measure of statistical significance. *P*-value cut-off used for computing statistical significance is < 0.05. *** in the figure refers to *P*-values ≤ 0.001 and ≤ 0.0001, respectively. Statistically non-significant comparisons are annotated as ns. Scale bar = 10 μm.

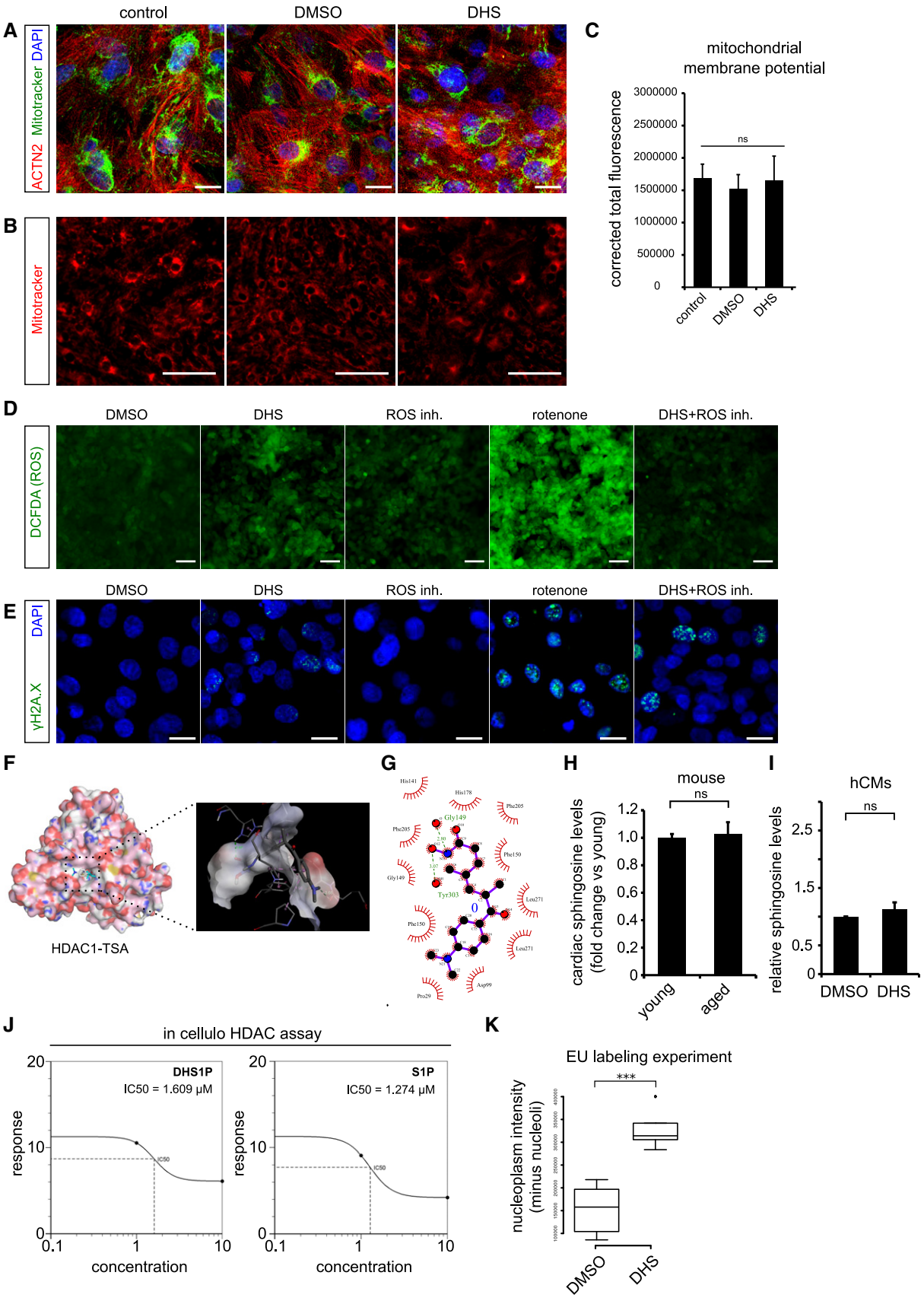

Figure EV4.